The true Cramer-Rao bound for estimating the carrier phase of a convolutionally encoded signal

Nele Noels, Heidi Steendam and Marc Moeneclaey
Telecommunications and Information Processing (TELIN) department, Ghent University,
St-Pietersnieuwstraat 41, B-9000 Gent, Belgium
{nnoels, Marc.Moeneclaey}@telin.rug.ac.be
Tel: ++32-9-264 34 12; Fax: ++32-9-264 42 95

Abstract -This contribution considers the *true* Cramer-Rao bound CRB related to estimating the carrier phase of a noisy linearly modulated signal in the presence of *encoded data* symbols. Timing delay and frequency offset are assumed to be known. A general expression and computational method is derived to evaluate the CRB in the presence of codes for which a trellis diagram can be drawn (block codes, trellis codes, convolutional codes,…). Results are obtained for several *minimum free distance non-recursive convolutional (NRC) codes*, and are compared with the CRB obtained with *random* (uncoded) data [1] and with the *modified* Cramer-Rao bound (MCRB) from [2]. We find that for small signal-to-noise ratio (SNR) the CRB is considerably smaller for coded transmission than for uncoded transmission. We show that the SNR at which the CRB is close to the MCRB decreases as the coding gain increases, and corresponds to a bit error rate (BER) of about 10^{-3}. We also compare the new CRBs with the simulated performance of (i) the (code-independent) Viterbi & Viterbi phase estimator [3] and (ii) the recently developed turbo synchronizer [4, 5].

I. Introduction

The Cramer-Rao bound (CRB) is a lower bound on the error variance of any unbiased estimate, and as such serves as a useful benchmark for practical estimators [6]. In many cases, the statistics of the observation depend not only on the parameter to be estimated, but also on a nuisance (vector) parameter we do not want to estimate. The presence of this nuisance parameter makes the analytical computation of the CRB very hard, if not impossible.

In order to avoid the computational complexity caused by the nuisance parameters, a 'modified' CRB (MCRB) has been derived in [2]. The MCRB is much simpler to evaluate than the CRB, but is in general looser than the CRB. In [7], the high-SNR limit of the CRB related to estimating a scalar synchronization parameter has been evaluated analytically; and has been shown to coincide with the MCRB in case of a discrete nuisance vector parameter. In the presence of coding, synchronization algorithms must operate at low SNR, so that the high-SNR limit of the CRB might no longer be a relevant benchmark.

The 'true' (as opposed to the 'modified') CRB related to carrier phase estimation has been derived assuming *uncoded* transmission, for BPSK and QPSK in [1] and for general symmetric QAM in [8]. In [9], the low-SNR limit of the CRB for carrier phase estimation, has been obtained analytically for *uncoded* PSK, QAM and PAM constellations. In this contribution we further investigate the true CRB for the estimation of the carrier phase of a noisy linearly modulated signal *in the presence of coding*. In section III a general expression and computational method is derived to evaluate the CRB in the presence of codes for which a trellis diagram can be drawn. Section IV considers the low-SNR limit of this CRB. Simulation results are provided in section V for maximum free-distance *non-recursive* convolutional (NRC) codes (r,n) with rate $r \in \{½, ¼\}$ and $n \in \{2, 4, 16, 64\}$ states, and BPSK and QPSK constellations (section A). Also, the simulated performance of the classical (code-independent) Viterbi & Viterbi phase estimator [3] and of the turbo synchronizer [4,5], operating on (½, 16)-convolutionally encoded QPSK signals, is compared with the corresponding CRB (section B). Sections VI concludes this paper.

II. Problem formulation

Consider a linearly modulated signal, obtained by applying a convolutionally encoded data symbol sequence to a square-root Nyquist transmit filter, that is transmitted over an additive white Gaussian noise (AWGN) channel. The resulting noisy signal is applied to a receiver filter, matched to the transmit filter. The receiver filter output signal is sampled at the correct decision instants, which yields the observation vector $\mathbf{r}=(r_{-K},\ldots,r_K)$, with

$$r_k = e\, a_k \exp(jq) + w_k \qquad (1)$$

for k = -K, …, K. In (1), $\{a_k\}$ is a sequence of L = 2K+1 data symbols taken from an M-PSK, M-PAM or M-QAM constellation ($E[|a_k|^2]=1$) according to a combination of an encoding rule and a mapping rule. The sequence $\{w_k\}$ consists of independent identically distributed (iid) zero-mean complex Gaussian noise variables, with independent real and imaginary parts each having a variance of ½. The deterministic unknown parameter θ represents the carrier phase. Finally, $\varepsilon = (E_s/N_0)^{1/2}$, with E_s and N_0 denoting the energy per coded symbol and the noise power spectral density, repectively.

Suppose that one is able to produce from the observation vector $\mathbf{r}$ an *unbiased* estimate $\hat{\theta}$ of the deterministic parameter θ. Then the estimation error variance is lower bounded by the CRB: $E_{\mathbf{r}}[(\hat{\theta}-\theta)^2] \geq CRB$, where the CRB is the given by [6]

$$CRB = E_{\mathbf{r}}\left[\left(\frac{d}{d\theta}\ln(p(\mathbf{r};\theta))\right)^2\right]^{-1} \quad (2)$$

The probability density function $p(\mathbf{r};\theta)$ of $\mathbf{r}$, corresponding to a given value of θ, is called the *likelihood function* of θ, while $\ln(p(\mathbf{r};\theta))$ is the *log-likelihood function* of θ. The expectation $E_{\mathbf{r}}[.]$ in (2) is with respect to $p(\mathbf{r};\theta)$.

As the observation $\mathbf{r}$ depends not only on θ, but also on the data symbols $\mathbf{a}$, the likelihood function of θ is obtained by averaging the *joint* likelihood function $p(\mathbf{r}|\mathbf{a};\theta)$ of the vector $(\theta,\mathbf{a})$ over the a priori distribution of the data symbols: $p(\mathbf{r};\mathbf{u}) = E_{\mathbf{a}}[p(\mathbf{r}\,|\,\mathbf{a};\theta)]$. The log-likelihood function $\ln(p(\mathbf{r}|\theta))$ is, within a factor not depending on θ, given by

$$\ln(\,p\,(\mathbf{r};\theta)\,) = \ln\left(E_{\mathbf{a}}\left[\prod_{k=-K}^{K} F\left(a_k, r_k e^{-j\theta}\right)\right]\right) \quad (3)$$

where

$$F\left(a_k, r_k e^{-j\theta}\right) = \exp\left(2\varepsilon \operatorname{Re}\left(a_k^* r_k e^{-j\theta}\right) - \varepsilon^2 |a_k|^2\right)$$

with r_k given by (1). Computation of the CRB requires the substitution of (3) into (2), and the evaluation of the various expectations included in (3) and (2).

As the evaluation of the expectations involved in (3) and (2) is quite tedious, a simpler lower bound, called the modified CRB (MCRB), has been derived in [2], i.e., $E_{\mathbf{r}}[(\hat{\theta}-\theta)^2] \geq CRB \geq MCRB$. The MCRB for phase estimation, is given by

$$MCRB = \frac{1}{2L\dfrac{E_s}{N_0}} \quad (4)$$

Since the computation of the MCRB makes no specific assumptions regarding the correlation between the data symbols, (4) is valid for uncoded as well as coded transmission, regardless of the encoding rule. In [7] an expression has been derived for the high-SNR limit of the CRB (2), and has been shown to coincide with the MCRB (4). Also, a closed-form expression can be derived for the *low*-SNR limit (i.e. $E_s/N_0 \to 0$) of the CRB, which we call the asymptotic CRB (ACRB). In [9] this has been accomplished for the CRB related to carrier phase estimation assuming uncoded data symbols, taken independently from a PAM, PSK or QAM constellation. The ACRB for coded data symbols can be computed in a similar way (see section IV). The true CRB related to carrier phase estimation has been derived assuming *uncoded* transmission, for BPSK and QPSK in [1] and for general symmetric QAM in [8]. Note that, in the presence of coding, the evaluation of (3) becomes even more complex since the data symbols are no longer independent identically distributed (iid). In this contribution we further investigate the true CRB for the estimation of the carrier phase of a noisy linearly modulated signal *in the presence of coding*.

III. Evaluation of the true CRB

We obtain for the log-likelihood function $\ln(p(\mathbf{r}|\theta))$ from (3)

$$\ln(p(\mathbf{r};\theta)) = \ln\left(\sum_{i=0}^{M^L-1} \Pr[\mathbf{a} = \mathbf{c}_i] \prod_{k=-K}^{K} F\left(c_{i,k}, r_k e^{-j\theta}\right)\right) \quad (5)$$

where $\mathbf{c}_i=(c_{i,-K},\ldots,c_{i,K})$. Denoting by ξ the set of legitimate coded sequences of length L, we have $\Pr[\mathbf{a} = \mathbf{c}] = M^{-rL}$ for $\mathbf{c}\in\xi$ and $\Pr[\mathbf{a} = \mathbf{c}] = 0$ otherwise, with r and M denoting the rate of the code and the constellation size, respectively. Differentiating with respect to θ yields, after some manipulations,

$$\frac{d}{d\theta}\ln\left(p\left(\mathbf{r};\theta\right)\right) = 2\varepsilon \sum_{k=-K}^{K}\sum_{i=0}^{M-1} p\left(a_k = \alpha_i \,|\, \mathbf{r};\theta\right) \operatorname{Im}\left(\alpha_i^* r_k e^{-j\theta}\right)$$

where $(\alpha_0, \alpha_1, ..., \alpha_{M-1})$ is the set of constellation points, and $p\left(a_k = \alpha_i \,|\, \mathbf{r};\theta\right)$ is the *marginal a postiori probability* of the k^{th} transmitted symbol. Substituting (6) into (2) yields

$$CRB_\theta^{-1} = 4\,\varepsilon^2 \left(\sum_{k=-K}^{K}\sum_{i=0}^{M-1} p\left(a_k = \alpha_i \,|\, \mathbf{r},\theta\right) \operatorname{Im}\left(\alpha_i^* r_k e^{-j\theta}\right)\right)^2 \quad (7)$$

For codes for which a coding trellis can be drawn (such as convolutional codes), the probabilities $p\left(a_k = \alpha_i \,|\, \mathbf{r},\theta\right)$ are easily computed by means of the BCJR algorithm [10].

IV. Low-SNR limit of the true CRB

As in [9] we can derive an expression for the low-SNR limit of the CRB by expanding the exponential function in (3) into a Taylor series and averaging each resulting term with respect to the data symbols. This yields

$$p\,(\mathbf{r}\,|\,\theta) = 1 + \sum_{i=1}^{\infty} A_i(\mathbf{r},\theta)\,\varepsilon^i \quad (8)$$

The quantities $A_i(\mathbf{r},\theta)$ depend on moments of the coded symbols of the type $E\left[a_{k_1}\ldots a_{k_n} a_{k_{n+1}}^* \ldots a_{k_i}^*\right]$. For codes that are described by means of a trellis, these moments can be computed based on the Markov property. For small E_s/N_0, we keep in the summation over i in (8) only the term with $i=i_0$, where i_0 is the smallest index i for which $dA_i(\mathbf{r},\theta)/d\theta$ is nonzero. Hence, $\ln p(\mathbf{r};\theta) \approx A_{i_0}(\mathbf{r},\theta)\,\varepsilon^{i_0}$, which after substitution in (2) yields a CRB that is proportional to $(E_s/N_0)^{-i_0}$.

Provided that the moments of the coded symbols involved in $A_i(\mathbf{r},\theta)$ with $i = 1, ..., i_0$ and $dA_i(\mathbf{r},\theta)/d\theta \neq 0$ are the same as for uncoded symbols, the ACRB reduces to the ACRB for uncoded transmission, derived in [9]. A similar reasoning as in [11, 12] can be followed to derive sufficient conditions on

the trellis and its branch labels, yielding an ACRB that is the same as for uncoded transmission. We have verified that many good convolutional codes satisfy these conditions, assuming that the trellis states at the beginning and the end of the observation interval are equally likely (so that all trellis state probabilities assume their steady state values). However, when the trellis state at the beginning and/or end of the observation interval is fixed, these conditions might no longer be satisfied, so that the ACRBs corresponding to coded and uncoded operation differ nevertheless.

V. Numerical results and discussion

A. *CRB_q from convolutionally encoded data symbols*

Analytical evaluation of the CRB (7) is extremely difficult, if not impossible; therefore we resort to computer simulation. We focus on maximum free-distance convolutional codes (r,n) (see Table I), which are optimal for BPSK and QPSK constellations with Gray mapping. Here, r denotes the code rate and n denotes the number of states.

Observation length and code termination

Fig. 1 illustrates some effects of a (½, 4) code on the ratio CRB/MCRB, assuming L transmitted QPSK symbols. The results for uncoded transmission and for two encoding scenarios are displayed, for different values of the observation length L. Scenario (i) corresponds to equally likely states at the beginning and end of each observation interval. In scenario (ii) each L symbol sequence **a** starts and ends in the zero state. It follows from Fig. 1 that:

- For low SNR the ratio CRB/MCRB converges to the corresponding ACRB/MCRB. Scenario (i) yields the same ACRB as uncoded transmission, i.e., proportional to $(E_s/N_0)^{-4}$, which corresponds to $i_0 = 4$. For scenario (ii) we find $i_0=2$, and the corresponding ACRB is only proportional to $(E_s/N_0)^{-2}$.
- For scenario (ii), the ratio ACRB/MCRB increases proportionally with L. This indicates that the ACRB is L-independent, which can easily be verified.
- For both scenarios the ratio CRB/MCRB decreases as L increases.
- For moderate and high values of L, both the effect of observation length and the effect of the termination are very small. This can be motivated as follows: whenever the transmitted sequences are long as compared to $\log_2(n)$, the effect of any fixed starting and/or ending state, and the effect of worse performance of the code at the edges of the transmission interval will be negligible

Code rate and number of states

Fig. 2 (QPSK) and Fig. 3 (BPSK) depict the ratio CRB/MCRB as a function of the ratio E_s/N_0 per coded symbol, for several (see Table I) maximum free distance convolutional (r,n) codes with $r \in \{½, ¼\}$ and $n \in \{2, 4, 16, 64\}$. The output of the encoder is Gray mapped onto the QPSK/BPSK symbols. We will assume that transmitted sequences are long as compared to $\log_2(n)$. The result for uncoded transmission is also displayed. Our results show that

- The ratio CRB/MCRB for SNR below (above) a certain cross-over region increases (decreases) when the number of states increases.
- Decreasing the code rate shifts the cross-over region to smaller SNR values, and hence enlarges the SNR region in which the ratio CRB/MCRB decreases with n.
- For small SNR, the CRB is considerably smaller for coded transmission than for uncoded transmission. This indicates that it is potentially more accurate to estimate θ from coded data than from uncoded data; the accuracy increases as the coding gain becomes larger.
- For very large E_s/N_0 the CRB converges to the MCRB.

TABLE I:
GENERATORS IN OCTAL FOR (r, n) MAXIMUM FREE DISTANCE CONV. CODES [10]

n\r	1/2	1/4
2	3 1	-
4	5 7	5 7 7 7
16	23 35	25 27 33 37
64	133 171	135 135 147 163

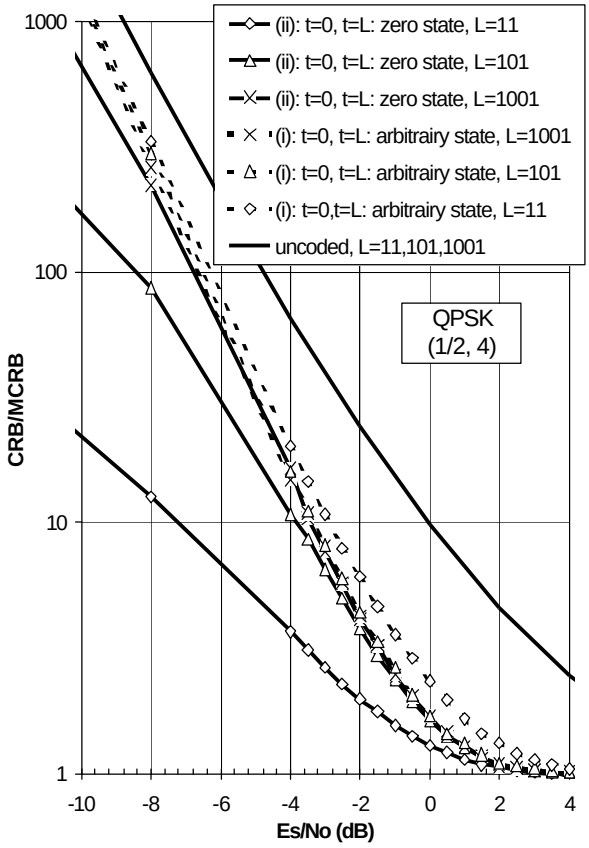

Fig. 1: Effects of observation length and code termination on the ratio CRB/MCRB fpr the (1/2, 4) NRC code (Table I)

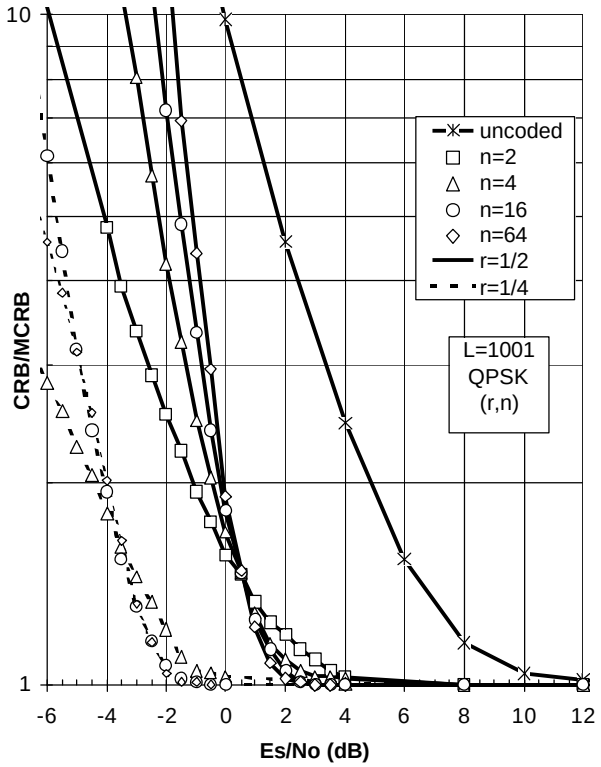

Fig.2: The ratio CRB/MCRB for a QPSK constellation and several maximum free distance (r, n) convolutional codes

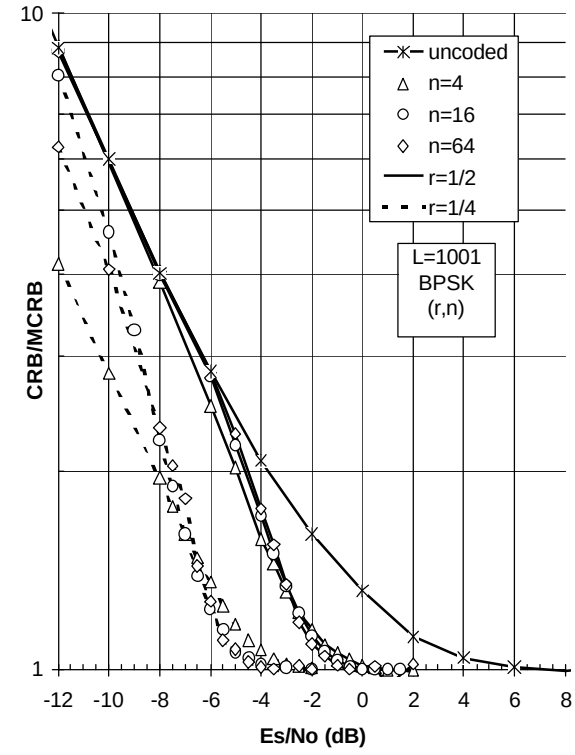

Fig. 3: The ratio CRB/MCRB for a BPSK constellation and several maximum free distance (r, n) convolutional codes

- For very small E_s/N_0 the CRB converges to the corresponding ACRB.
  - For QPSK, the codes with *rate ½* all yield the same ACRB as in the uncoded case except for n=2, which yields an ACRB proportional to $(E_s/N_0)^{-3}$. For *rate ¼*, none of the codes yields the same ACRB as in the uncoded case. For n=4 or n=64 we obtain an ACRB proportional to $(E_s/N_0)^{-2}$; basically, this is because not all four generators are different (see table I). The code (¼,16) yields an ACRB proportional to $(E_s/N_0)^{-4}$, parallel but not equal to the ACRB for uncoded transmission.
  - For BPSK, all codes yield the same ACRB as in the uncoded case, except for the codes (¼,4) and (¼,64), that yield an ACRB parallel to the one for uncoded transmission.
- As the constellation size increases from M=2 to M=4 the CRB at a fixed Es/N_0 increases, and the value at which the CRB is close to the MCRB shifts to the left by about 3dB. This indicates that at low SNR, phase estimation is more difficult for QPSK than for BPSK.

Fig. 4 shows the BER, resulting from MAP decoding of the considered codes, as a function of E_s/N_0 per coded QPSK symbol. The BER for uncoded QPSK transmission is also displayed.

- Note the cross-over region, in correspondence with the one in Fig. 1 for the CRB/MCRB curves. The BER for SNR below (above) a cross-over region increases (decreases) when the number of states increases. A possible explanation for this phenomenon is that for very small SNR not the free distance (decreasing with n) but the number of nearest neighbors (increasing with n) becomes determinating for the BER performance of the code.
- We can motivate now the departure of the CRB from the MCRB. For *uncoded* transmission the ratio CRB/MCRB becomes close to one at values of SNR that yield a BER less than about 10^{-3}. Our results show that for *coded* transmission the "knee point" of the CRB/MCRB curves is also located at that SNR value where BER $\approx 10^{-3}$.
- As compared to a QPSK constellation, a BPSK constellation yields the same BER performance at a 3 dB lower E_s/N_0. This explains the 3 dB shift of the "knee point" (Fig. 3 versus Fig. 2)

B. *Comparison of the CRB with the performance evaluation of NDA phase estimators*

To estimate the carrier phase of the received vector (1), we consider two algorithms:

(i) The classical NDA algorithm proposed in [3] and referred to as V & V estimators, for which estimates are obtained as

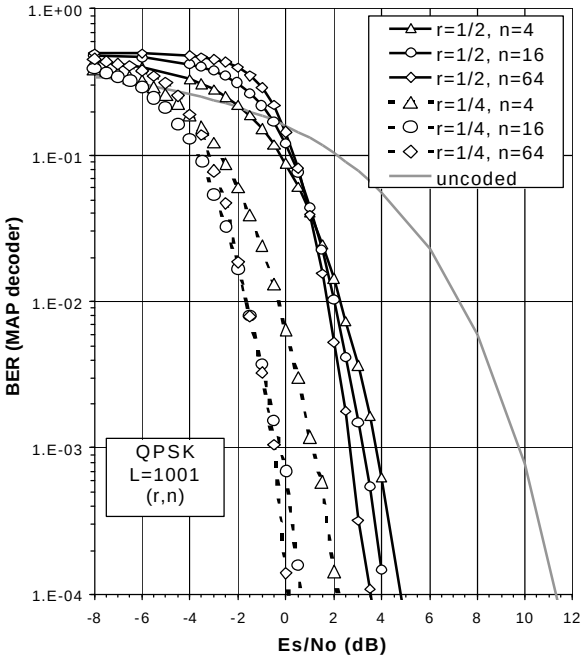

Fig. 4: BER as obtained with a MAP decoder

$$\hat{\theta} = \frac{1}{M} \arg\left\{ \sum_{k=-K}^{K} |r_k|^X \, e^{jM \arg\{r_k\}} \right\} \qquad (9)$$

We chose X=2, since it is indicated in [3] that for QPSK signals, the monomial $|r_k|^2$ is nearly optimal in the sense of providing estimates (9) with the lowest variance.

(ii) The iterative turbo phase estimator technique as recently developed in [4] for turbo codes and justified and generalized in [5], for which estimates are iteratively obtained as

$$\hat{\theta}^{(n)} = \arg\left\{ \sum_{k=-K}^{K} r_k \sum_{i=0}^{M-1} P\left(a_k = \alpha_i \,\middle|\, \mathbf{r}, \hat{\theta}^{(n-1)}\right) \alpha_i^* \right\} \qquad (10)$$

where $\hat{\theta}^{(0)} = 0$. In the nth decoding iteration step the mached filter output samples are pre-corrected in phase over $\hat{\theta}^{(n-1)}$, soft decision is performed for all symbols (i.e. $P\left(a_k = \alpha_i \,\middle|\, \mathbf{r}, \hat{\theta}^{(n-1)}\right)$) using the BCJR algorithm, and the nth phase estimate $\hat{\theta}^{(n)}$ is computed according to (9). The final value of $P\left(a_k = \alpha_i \,\middle|\, \mathbf{r}, \hat{\theta}\right)$ can then be used to produce MAP-decoding on the received encoded signal.

Note that algorithm (i) does not take the coding into account, this is in contrast with algorithm (ii) which does take full advantage of the code structure.

Fig. 5 shows the simulated *mean estimated value* (MEV) and Fig. 6 the *mean square estimation error* (MSEE) obtained with algorithm (i) and algorithm (ii), as a function of the ratio E_s/N_0 per coded symbol. For the turbo synchronizer results are presented for 1, 2 and 10 iterations of the turbo synchronizer. Each simulation consisted on processing 10^6 blocks of L=1001 (½, 16) NRC encoded symbols each, using QPSK modulation and a carrier phase offset of 0.2 rad. The relevant CRBs are also displayed. Our results show that

- The V&V estimator produces an unbiased estimate up to values of SNR as low as –1dB. In this SNR-region the MSEE is much larger than the true CRB (7), but approaches the CRB for uncoded transmission [1] very closely. Indeed, as the V&V estimatior (9) does not take advantage of the code structure, its MSEE is lower bounded by the CRB for uncoded transmission. The good performance as compared to the CRB for uncoded transmission is a result of the large observation length L.
- For a fixed value of E_s/N_0, the turbo synchronizer structure produces estimates with gradually increasing performance and decreasing bias, as the number of synchronizer iterations increases. After 10 iterations the estimate is unbiased up to 0dB, and the true CRB (7) for a (½, 16) NRC code is reached.

VI. Conclusions

In this contribution we have expressed the true CRB for carrier phase estimation in terms of the a posteriori probability of the data symbols. This allows to evaluate the CRB in the case of coded data symbols, when the code is described by means of a trellis. Also the low-SNR limit of the CRB has been determined.

Through computer simulations we have obtained numerical results for the CRB related to the estimation of the

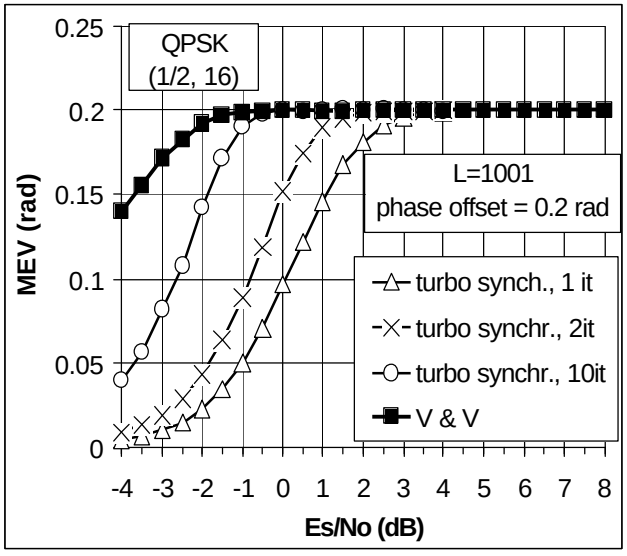

Fig. 5: MEV of V&V estimator and turbo estimator with 1, 2 and 10 iterations and observation length = 1001 symbols operating on a (½ , 16) NRC encoded QPSK signal with carrier phase offset of 0.2 rad

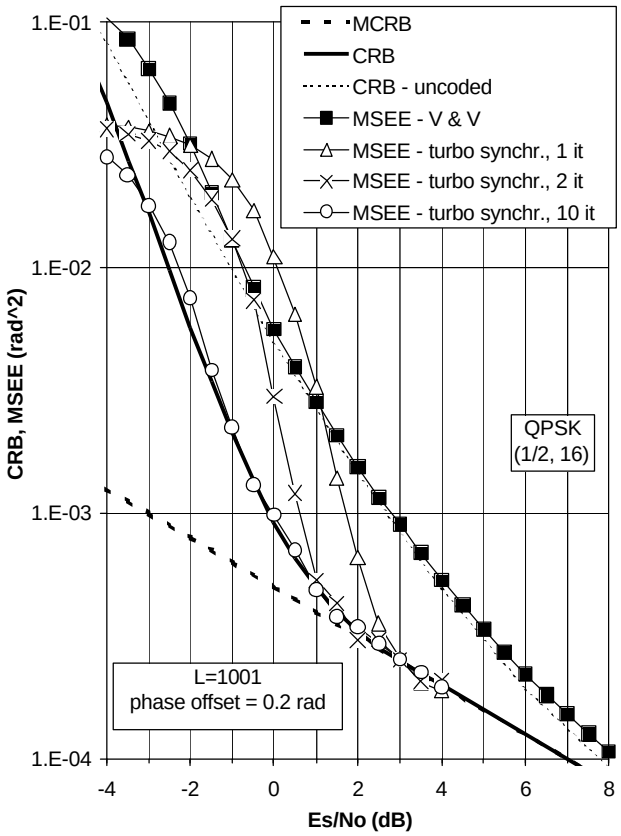

Fig. 6: MSEE of V&V estimator and turbo estimator with 1, 2 and 10 iterations and observation length = 1001.operating on a (½ , 16) NRC encoded QPSK signal with carrier phase offset 0.2 rad

phase offset of a linearly modulated signal in the presence of convolutionally encoded data symbols. We have pointed out that for sequences that are long as compared to the code memory the effect of a fixed initial or final state, and the effect of the observation length on the ratio CRB/MCRB is small. Further, our results indicate that estimating the phase from coded data is potentially more accurate than estimating it from non-coded data. This effect is more pronounced as the coding gain gets larger. It was shown that (in accordance with the result for uncoded transmission) the CRB is close to the MCRB for SNR values that yield a BER less than about 10^{-3}. Also, we have found that the MSEE performance of the iterative turbo synchronizer [4,5] reaches the CRB for a large number of synchronizer iterations.

Application of this method to block codes and turbo codes is straightforward and is a topic for further work.

ACKNOWLEDGEMENTS

The second author gratefully acknowledges the financial support from the Belgian National Fund for Scientific Research (FWO Flanders).

REFERENCES

[1] W.G. Cowley, "Phase and frequency estimation for PSK packets: Bounds and algorithms," IEEE Trans. Commun., vol. COM-44, pp. 26-28, Jan. 1996

[2] A.N. D'Andrea, U. Mengali and R. Reggiannini, "The modified Cramer-Rao bound and its applications to synchronization problems," IEEE Trans. Commun., vol. COM-24, pp. 1391-1399, Feb./Mar./Apr. 1994

[3] A. J. Viterbi and A. M. Viterbi, "Nonlinear estimation of PSK-modulated carrier phase with application to burst digital transmission," IEEE Trans. Inform. Theory, vol. IT-29, pp.543-551, July 1983.

[4] V. Lottici and M. Luise, "Carrier Phase Recovery for Turbo-Coded Linear Modulations," In Proc. IEEE ICC, May 2002, New York

[5] N. Noels, V. Lottici, A. Dejonghe, H. Steendam, M. Moeneclaey, M. Luise, L. Vandendorpe, "A Theoretical Framework for Soft Information Based Synchronization in Iterative (Turbo) Receivers," submitted to IEEE Trans. on Comm.

[6] H.L. Van Trees, Detection, Estimation and Modulation Theory. New York: Wiley, 1968

[7] M. Moeneclaey, "On the true and the modified Cramer-Rao bounds for the estimation of a scalar parameter in the presence of nuisance parameters," IEEE Trans. Commun., vol. COM-46, pp. 1536-1544, Nov. 1998

[8] F. Rice, B. Cowley, B. Moran, M. Rice, "Cramer-Rao lower bounds for QAM phase and frequency estimation," IEEE Trans. Commun., vol. 49, pp 1582-1591, Sep. 2001

[9] H. Steendam and M. Moeneclaey, "Low-SNR limit of the Cramer-Rao bound for estimating the carrier phase and frequency of a PAM, PSK or QAM waveform," IEEE Communications Letters, vol. 5, pp. 215-217, May 2001.

[10] L. R. Bahl, J. Cocke, F. Jelinek and J. Raviv, "Optimal decoding of linear codes for minimizing symbol error rate," IEEE Trans. Inf. Theory, pp 284-287, March 1974

[11] M. Moeneclaey and P. Sanders, "Close-to-optimum joint carrier and symbol synchronization for trellis coded two-dimensional modulation schemes," in Proc. IEEE ICC, June 1988, pp 1038-1042

[12] M. Moeneclaey and U. Mengali, "Sufficient conditions on trellis-coded modulation for code-independent synchronizer performance," IEEE Trans. Commun., vol. 38, No 5, pp 595-601, May 1990